Possible nodeless superconductivity in the noncentrosymmetric superconductor $Mg_{12-\delta}Ir_{19}B_{16}$

Gang Mu, Yue Wang, Lei Shan, and Hai-Hu Wen*

National Laboratory for Superconductivity, Institute of Physics and Beijing National Laboratory for Condensed Matter Physics, Chinese Academy of Sciences, P.O. Box 603, Beijing 100080, People's Republic of China

(Received 25 May 2007; published 22 August 2007)

We measured the resistivity, diamagnetization, and low-temperature specific heat of the newly discovered noncentrosymmetric superconductor $Mg_{12-\delta}Ir_{19}B_{16}$. The temperature dependence of specific heat is consistent with the model of an isotropic *s*-wave gap with value $\Delta_0 \approx 0.94$ meV for the sample $T_c = 5.7$ K, and the ratio $\Delta_0/k_BT_c \approx 1.91$ indicates a slightly moderate coupling for the superconductivity. The correlations among the normal state Sommerfeld constant γ_n, the slope $-d\mu_0 H_{c2}(T)/dT$ near T_c, and the condensation energy E_c are all consistent with the slightly moderate coupling picture. Based on the data of phonon contribution, T_c and the McMillan formula, we obtained an electron-phonon coupling strength $\lambda_{e\text{-ph}} \approx 0.66$, which suggests that the superconductivity here is induced by the electron-phonon coupling.

DOI: 10.1103/PhysRevB.76.064527 PACS number(s): 74.20.Mn, 74.20.Rp, 74.25.Bt, 74.70.Dd

I. INTRODUCTION

The study on superconductivity in noncentrosymmetric materials has attracted growing efforts in recent years.[1–5] For most superconductors, the atomic lattice has a centrosymmetry, therefore the system is inversion symmetric. The orbital part of the superconducting order parameter has a subgroup which is confined by the general group of the atomic lattice. Due to the Pauli's exclusion rule and the parity conservation, the Cooper pair with orbital even parity should have antiparallel spin state, namely spin singlet, while those having orbital odd parity should have parallel spin state, i.e., spin triplet. If a system lacks the centrosymmetry, the enhanced spin-orbital coupling may promote the formation of pairing with high angular momentum, such as the triplet pairing. Meanwhile the noncentrosymmetric structure allows for the existence of a mixture of singlet and triplet pairing. Theoretical features are anticipated in the noncentrosymmetric system.[6] A nodal gap structure has been observed in Li_2Pt_3B showing the possibility of triplet pairing, while due to weaker spin-orbital coupling,[7,8] the nodal gap has not been observed in a material Li_2Pd_3B with similar structure. It is thus highly desired to investigate the pairing symmetry in more materials with noncentrosymmetric structure.

The newly discovered superconductor $Mg_{10}Ir_{19}B_{16}$ (hereafter abbreviated as MgIrB) (Ref. 9) with superconducting transition temperature $T_c \approx 5$ K is one of the rare materials which have the noncentrosymmetry. This material has a space group of $I\text{-}43m$ with large and complex unit cells of about 45 atoms. To some extent it resembles the system $Li_2(Pt,Pd)_3B$ since they have alkaline metals (Li, Mg), heavy transition elements (Pd, Pt, Ir), and the light element boron. Theoretically it was shown that the major quasiparticle density of states (DOS) derives from the *d* orbital of the heavy transition elements. In this paper we present a detailed investigation and analysis on the superconducting properties, such as the energy gap, pairing symmetry, electron-phonon coupling strength, condensation energy, etc., in MgIrB. Our results suggest that the superconductivity in this system is of the BCS type with an *s*-wave gap symmetry and a slightly moderate electron-phonon coupling strength.

II. SAMPLE PREPARATION AND CHARACTERIZATION

The samples were prepared in two steps starting from pure elements of Mg (98.5%), Ir (99.95%), and B (99.999%) using a standard method of solid state reaction. Appropriate mixtures of these starting materials were pressed into pellets, wrapped in Ta foil, and sealed in a quartz tube with an atmosphere of 95% Ar/5% H_2. The materials were then heated at 600 °C and 900 °C for 40 min and 80 min, respectively. After cooling down to room temperature, the samples were reground and then they were pressed into pellets and sealed in a quartz tube with the same atmosphere as used in the first step. Some of the time they were mixed with another certain amount of Mg up to 20%. In this process the sample was heated up to 900 °C directly and maintained for 80 min. Usually the superconducting transition becomes sharper after the second process, but sometimes the T_c may become slightly lower than the first time. The synthesizing process here is similar to the previous work reported by the Princeton group[9] but still with some differences. For example, we used Mg powder instead of flakes to make the mixture more homogeneous. In addition, the pressure in the sealed quartz tube may rise to nearly 4 atm at 900 °C, which may considerably reduce the volatilization of Mg during the synthesis. This is probably the reason that the sample with the transition temperature as high as $T_c = 5.7$ K was made without adding extra Mg in the second step with the starting ratio in the first step as Mg:Ir:B=12:19:16.

The resistivity and the ac susceptibility were measured based on an Oxford cryogenic system (Maglab-Exa-12). The specific heat was measured on the Quantum Design instrument physical property measurement system (PPMS) with temperature down to 1.8 K and the PPMS based dilution refrigerator (DR) down to 150 mK. The temperatures of both systems have been well calibrated showing consistency with an error below 2% in the temperature range from 1.8 K to 10 K.

As shown in Fig. 1, the x-ray diffraction (XRD) pattern taken on one sample with $T_c = 5.7$ K shows a single phase with very small amount of impurity which is comparable to that reported previously.[9] After the first round of synthesiz-

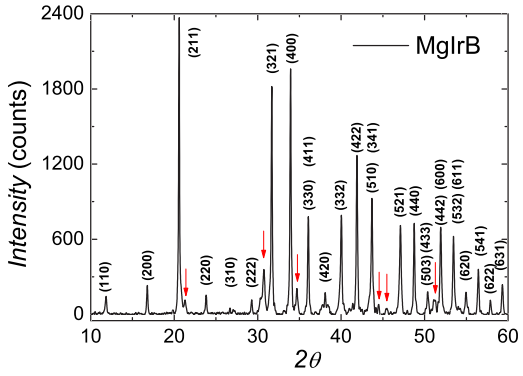

FIG. 1. (Color online) The x-ray diffraction pattern measured for the sample T_c=5.7 K. The peaks from the secondary impurity phase are marked by the arrows. It is clear that the main diffraction peaks are from the phase MgIrB.

ing, the superconducting transition inspected by the ac susceptibility occurs at about 5 K with a relatively wide transition. However, after the second step, the transition moves to about 5.7 K with a sharper transition width if we did not add extra Mg in the second step. The Ta foil seems unreacted with the materials in both steps of the fabrication if the Mg content is below 12 in the stoichiometric formula.

In the top frame of Fig. 2 we show the temperature dependence of resistivity under different magnetic fields. One can see that the transition width determined from resistive measurements (1%–99% ρ_n) is only about 0.2 K. This is consistent with the rather sharp magnetic transition as revealed by the ac susceptibility data shown in the bottom view of Fig. 2. By applying a magnetic field the transition shifts to lower temperatures quickly with a

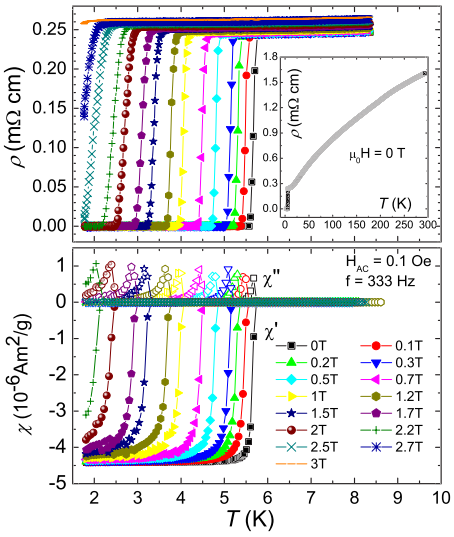

FIG. 2. (Color online) Temperature dependence of resistivity (top) and magnetic susceptibility (χ'' and χ') (bottom) under different dc magnetic fields. It is clear that the dc magnetic field makes the transition shift parallel to low temperatures, manifesting a field-induced pair-breaking effect. The inset in the top panel shows the resistive transition in a wide temperature regime at $\mu_0 H$=0 T.

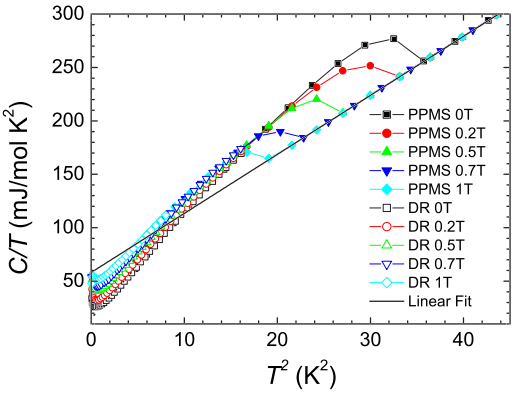

FIG. 3. (Color online) Raw data of specific heat plotted as C/T vs T^2. All filled symbols represent the data taken with PPMS at various magnetic fields. The open symbols show the data taken with the DR. The thick solid line represents the normal state specific heat which contains both the phonon and the electronic contributions.

slope $-d\mu_0 H_{c2}(T)/dT|_{T_c} \approx 0.63$ T/K for the present sample with T_c=5.7 K. Using the Werthamer-Helfand-Hohenberg relation[10] $\mu_0 H_{c2} = -0.69 d\mu_0 H_{c2}(T)/dT|_{T_c} T_c$, we get the upper critical field $\mu_0 H_{c2}$=2.48 T. The value found here is comparable to that reported in the earlier paper[9] ($T_c \approx 5$ K). It is interesting to note that the value of the slope $-d\mu_0 H_{c2}(T)/dT$ correlates strongly with T_c. For a sample with T_c=3.7 K, we found that $-d\mu_0 H_{c2}(T)/dT|_{T_c} \approx 0.2$ T/K. This suggests that there is a tunability of superconducting properties in this system which will be addressed in Sec. IV.

III. SPECIFIC HEAT AND FIT TO THE BCS MODEL

Shown in Fig. 3 are the raw data of the specific heat up to a magnetic field of 1 T. The open symbols represent the data taken with the DR, while all filled symbols show the data taken with the PPMS. Both sets of data coincide very well for different fields. With increasing the magnetic field the specific heat jump due to the superconducting transition moves quickly to lower temperatures leaving a background which is consistent with that above T_c at zero field. This provides a reliable way to extract the normal state specific heat as shown by the thick solid line since the normal state can be described by $C/T = \gamma_n + \beta T^2$, where the first and the second term correspond to the normal state electronic and phonon contribution, respectively. From the data it is found that β=5.4 mJ/mol K^4 and γ_n=57.7 mJ/mol K^2. By extrapolating the data in the superconducting state at zero field down to 0 K one finds, however, a residual value $\gamma_0 \approx 13.8$ mJ/mol K^2, indicating a contribution either by a nonsuperconducting fraction in volume of about 24%, or by the DOS induced by the impurity scattering for a nodal gap which will be discussed later. The residual γ_0 may be induced by the nonsuperconducting region, but it is still difficult to be regarded as due to an impurity phase with completely different structure as MgIrB since the XRD data shown in Fig. 1 is quite clean. We thus suggest that the superconductivity depends sensitively on the relative compositions among the three elements and some regions without

superconductivity have the chemical composition and even the structure close to the superconducting phase. In any case, it is safe to conclude that the normal state Sommerfeld constant for the present sample is close to or slightly above 43.9 mJ/mol K^2.

Next we can have an estimation on the electron-phonon coupling strength based on γ_n. In MgIrB, the electronic conduction is dominated by the 5d band electrons of Ir atoms. The DOS at E_F given by the local-density approximation band-structure calculation[11] is about $N(E_F)=5.51$/eV spin. By assuming that there is an electron-phonon coupling constant $\lambda_{e\text{-ph}}$ in the system, one has

$$\gamma_n = \frac{2\pi^2}{3} N(E_F) k_B^2 (1 + \lambda_{e\text{-ph}}). \quad (1)$$

Using the band-structure value of $N(F_F)$, we have $\gamma_n=25.98(1+\lambda_{e\text{-ph}})$(mJ/mol K^2). Taking the experimental value $\gamma_n=43.9$ mJ/mol K^2, we obtain $\lambda_{e\text{-ph}}\approx 0.68$, indicating a slightly moderate electron-phonon coupling.

In the raw data shown in Fig. 3, one can see an upturn of $\gamma=C/T$ in the very low-temperature region. This upturn is known as the Schottky anomaly, induced by lifting the degeneracy of the states of the paramagnetic spins. We tried a two level ($S=1/2$) model to fit the low-temperature data but found a poor fitting together with an extremely large Landé factor g in the Zeeman energy $g\mu_B H_{\text{eff}}$, where μ_B is the Bohr magneton, $H_{\text{eff}}=\sqrt{H^2+H_0^2}$ is the effective magnetic field which evolves into $H_{\text{eff}}=H_0$, the crystal field at zero external field. In MgIrB the most possible paramagnetic centers may be from Ir^{4+}($S=5/2$) or Ir^{3+}($S=2$). The system energy due to Zeeman splitting in a magnetic field is[12]

$$E_{\text{Sch}} = \sum E_i \exp(-E_i/k_BT) \Big/ \sum \exp(-E_i/k_BT), \quad (2)$$

where $E_i=M_J g\mu_B H_{\text{eff}}$ and $M_J=-S,-S+1,\ldots,S-1,S$. The specific heat due to the Schottky effect is thus $C_{\text{Sch}}=(n/k_B)dE_{\text{Sch}}/dT$, where n represents the concentration of the paramagnetic centers. For $S=5/2$ and $S=2$ the calculated results are very close to each other, therefore we show only the fit with $S=5/2$ corresponding to Ir^{4+} (six levels). This method allows us to deal with the data at zero and finite fields simultaneously. It is known that the Schottky term should be zero at $T=0$ K. In the superconducting state, the total specific heat can be written as $C_{\text{tot}}=C_{\text{nons}}+C_e+C_{\text{ph}}+C_{\text{Sch}}$ with $C_{\text{nons}}=\gamma_0 T$ as the contribution of the nonsuperconducting regions, C_e is the electronic part. In the zero temperature limit only the contribution of the nonsuperconducting part is left. Applying a magnetic field gives rise to a finite value $\Delta\gamma_e$ to $C_e=\gamma_e T$ due to the presence of vortices. Practically, in order to fit the Schottky term, we first remove the phonon contribution $C_{\text{ph}}=\beta T^3$, then vertically move the experimental data downward with a magnitude $\gamma_0=13.8$ mJ/mol K^2 and a field-induced vortex term $\Delta\gamma_e(H)$. In Fig. 4(a) we present the specific heat coefficient $\gamma_e-\gamma_n$ measured at the magnetic fields up to 1 T. An upturn due to the Schottky effect is visible in the low-temperature region for all fields. In Fig. 4(b) we show the data at $\mu_0 H=0$ T before [(red) filled circles] and after (dark open squares) removing the Schottky anomaly calculated

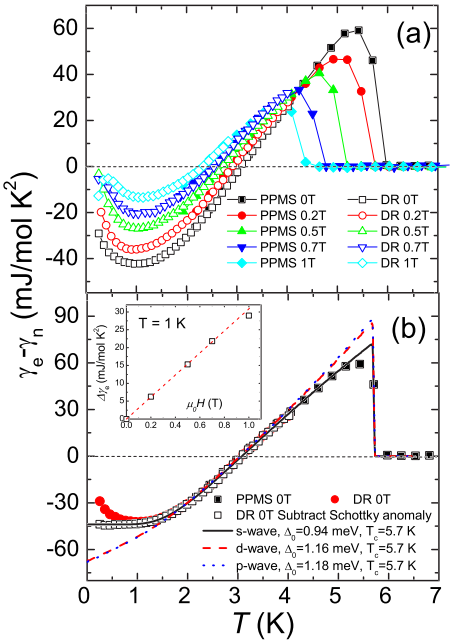

FIG. 4. (Color online) Temperature dependence of $\gamma_e-\gamma_n$ for (a) magnetic fields up to 1 T and (b) at zero field before (filled circles) and after removing (open and filled squares) the Schotkky anomaly. The dark solid, red dashed, and dotted green lines in (b) are the theoretical curves calculated based on the BCS model (see text) with a gap of s wave, d wave, and p wave, respectively.

based on the model of six levels with $\mu_0 H_0=0.25$ T, $n=3.74$ mJ/mol K, and $g=2$. Note that we used the value 43.9 mJ/mol K^2 as the normal state Sommerfeld constant γ_n. One can see that the low-temperature part after removing the Schottky anomaly is flattened out below about 0.8 K when the field is zero. Furthermore, it can also be justified by the requirement of entropy conservation. Since the Schottky term gives only a very small contribution in the high-temperature region (above 1.5 K here), if γ_e had a power law as required by a nodal gap, instead of a flat temperature dependence for an s-wave gap, the entropy would be clearly not conserved yielding a large negative entropy. This is of course unreasonable. In Fig. 4(b) we present together the theoretical curves for $\gamma_e-\gamma_n$ calculated using the weak coupling BCS formula

$$\gamma_e = \frac{4N(0)}{k_BT^3} \int_0^{\hbar\omega_D} \int_0^{2\pi} \frac{e^{\zeta/k_BT}}{(1+e^{\zeta/k_BT})^2} \times \left(\varepsilon^2 + \Delta^2(\theta,T) - \frac{T}{2}\frac{d\Delta^2(\theta,T)}{dT} \right) d\theta d\varepsilon, \quad (3)$$

where $\zeta=\sqrt{\varepsilon^2+\Delta^2(T,\theta)}$. In obtaining the theoretical fit we take the implicit relation $\Delta_0(T)$ derived from the weak coupling BCS theory for superconductors with different pairing symmetries: $\Delta(T,\theta)=\Delta_0(T)$ for s wave, $\Delta(T,\theta)=\Delta_0(T)\cos 2\theta$ for d wave, and $\Delta(T,\theta)=\Delta_0(T)\cos\theta$ for p wave, respectively. The theoretical curve of the s wave fits the experimental data very well leading to an isotropic gap value $\Delta_0=0.94$ meV and $T_c=5.7$ K. The ratio Δ_0/k_BT_c

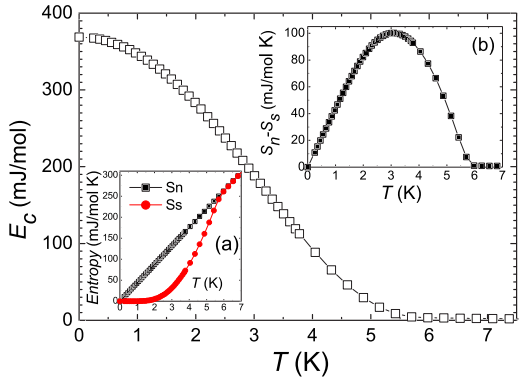

FIG. 5. (Color online) The main frame shows the superconducting condensation energy calculated from the specific heat. Inset (a) shows the entropy in the normal and superconducting state. Plotted in inset (b) is the difference of the entropy between the normal and superconducting state.

$=1.91$ obtained here is quite close to the prediction for the weak coupling limit ($\Delta_0/k_BT_c=1.76$), indicating a slightly moderate coupling strength. This is self-consistent with the conclusion derived from the estimation on γ_n. In addition, the specific heat anomaly at T_c is $\Delta C_e/\gamma_n T|_{T_c}\approx 1.64$ being close to the theoretical value 1.43 predicted for the case of weak coupling, again showing a slightly moderate coupling. The inset in Fig. 4(b) shows a field induced part $\Delta\gamma_e$. In an s-wave superconductor $\Delta\gamma_e$ is mainly contributed by the vortex cores and a linear relation $\Delta\gamma_e \propto H\gamma_n/H_{c2}(0)$ is anticipated[13] in the low field region with $\Delta_0^2/E_F \ll T \ll T_c$. This linear relation is well demonstrated by the data below 0.7 T, indicating another evidence of s-wave pairing symmetry. This is in sharp contrast with the results in cuprates where a $\Delta\gamma_e \propto \sqrt{H}$ relation is expected due to the Doppler shift of the nodal quasiparticle spectrum in a d-wave superconductor.[14,15] The theoretical curves calculated with d-wave and p-wave models cannot describe the data in both the low-temperature and high-temperature regimes.[13,16]

In the following we try to estimate the superconducting condensation energy E_c for the sample with $T_c=5.7$ K. In calculating E_c we get the entropy difference between the normal state and the superconducting state by $S_n-S_s=\int_0^T(\gamma_n-\gamma_e)dT'$, then E_c is calculated through $E_c=\int_T^{6\ \mathrm{K}}(S_n-S_s)dT'$. The data of S_n and S_s as well as the difference between them are shown in insets (a) and (b) of Fig. 5, respectively. The main frame of Fig. 5 shows the temperature dependence of the condensation energy E_c which is about 369 mJ/mol at $T=0$ K. This value can actually be assessed by the following equation:

$$E_c = \alpha N(E_F)\Delta_0^2/2 = \alpha\frac{3}{4\pi^2}\frac{1}{k_B^2}\gamma_n\Delta_0^2. \tag{4}$$

For a BCS s-wave superconductor, $\alpha=1$, taking $\gamma_n=43.9$ mJ/mol K^2 and $\Delta_0=0.94$ meV, we found a value of $E_c\approx 367$ mJ/mol which is remarkably close to the experimental value 369 mJ/mol. This also validates the values of Δ_0 and γ_n determined in our experiment.

Now we discuss the possibility of impurity scattering which may suppress the spin-triplet component of the superconductivity. Theoretically it is known that the nodal gap structure is very sensitive to the impurities. If the spin-singlet and triplet components are mixed, the latter might be suppressed by the impurity scattering and the system would behave like a BCS superconductor. Although we cannot exclude this possibility at this moment, it is safe to conclude that the spin-triplet component (if it exists) should be a very small part of the total condensate. This can be justified by the following two arguments. First, for the sample with $T_c=5.7$ K, we found that $\gamma_0/\gamma_n(T>T_c)=24\%$. Assuming that the total γ_0 were induced by the impurity scattering of this spin-triplet component, the ratio of the DOS corresponding to the normal state of this part would be less than 24%. Actually one would not expect that the total value of γ_0 here could be ascribed completely to the suppressed spin-triplet component since the XRD data does show the existence of some secondary (nonsuperconducting) phase which will certainly contribute a certain value of DOS. Second, the self-consistency among the derived values of the normal state Sommerfeld constant, the appropriate ratio of Δ_0/k_BT_c and the electron-phonon coupling strength (see next section) together with the nice fit of the specific heat data to the BCS model all can push the spin-triplet component to a very low limit. Nevertheless, as a future work it is worthwhile to have an inspection on this issue on a sample with complete purity.

IV. ELECTRON-PHONON COUPLING STRENGTH AND THE TUNABILITY OF SUPERCONDUCTIVITY IN MgIrB

Now we get to the electron-phonon coupling in MgIrB. From the normal state value we have derived the phonon contribution $C_{\mathrm{ph}}=\beta T^3$ with $\beta\approx 5.4$ mJ/mol K^4. Using the relation $\Theta_D=(12\pi^4 k_B N_A Z/5\beta)^{1/3}$, where $N_A=6.02\times 10^{23}$ is the Avogadro constant, $Z=45$ is the number of atoms in one unit cell, we get the Debye temperature $\Theta_D(\mathrm{MgIrB})=253$ K for the sample with $T_c=5.7$ K. If the conduction electrons are weakly coupled with the phonon, one can use the McMillan equation to evaluate the electron-phonon coupling strength $\lambda_{e\text{-ph}}$ via[17]

$$T_c = \frac{\Theta_D}{1.45}\exp\left(-\frac{1.04(1+\lambda_{e\text{-ph}})}{\lambda_{e\text{-ph}}-\mu^*(1+0.62\lambda_{e\text{-ph}})}\right), \tag{5}$$

where μ^* is the Coulomb pseudopotential taking 0.11. Using $\Theta_D(\mathrm{MgIrB})=253$ K and $T_c=5.7$ K, we obtain $\lambda_{e\text{-ph}}=0.66$, indicating a slightly moderate coupling strength. The value determined here is quite close to $\lambda_{e\text{-ph}}=0.68$ which was determined previously based on the comparison between the normal state Sommerfeld coefficient γ_n and the theoretically estimated DOS at E_F. All these detailed and self-consistent analysis indicate an electron-phonon coupling mechanism for superconductivity in MgIrB.

At this moment, it is still unclear that the conduction electrons are strongly coupled to which phonon branch leading to the superconductivity. During the preparation of samples, it was found that the superconducting transition temperature is

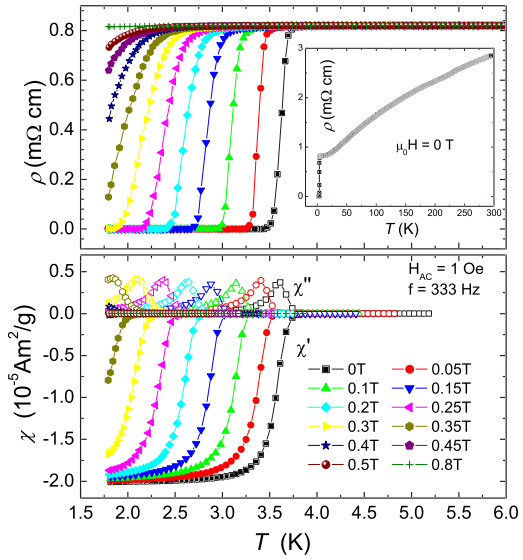

FIG. 6. (Color online) Temperature dependence of resistivity (top) and magnetic susceptibility (χ'' and χ') (bottom) under different dc magnetic fields for the sample with T_c=3.7 K. It is clear that the dc magnetic field makes the transition shift parallel to low temperatures with a much faster speed compared with the sample with T_c=5.7 K.

changeable in a wide regime (from 2 K to 5.7 K) in MgIrB with a rather sharp transition width. This is actually a rare case in the alloy superconductors in which the off-stoichiometric elements normally play as the scatterers and break the Cooper pairs and finally make the transition broad. In MgIrB a slight off-stoichiometry may not change the structure, but promote the mutual-substitution leading to a different electron-phonon coupling strength. In Fig. 6 we show the temperature dependence of the resistivity and the ac susceptibility of another sample (T_c=3.7 K) which was made also in two steps but with 20% more Mg added in the second step. One can see that the transition width at zero field is still quite narrow and the x-ray diffraction pattern taken on this sample is reasonably clean (not shown here). An estimation on the electron-phonon coupling strength $\lambda_{e\text{-ph}}$ based on the McMillan equation on this sample tells that $\lambda_{e\text{-ph}} \approx 0.55$. In Fig. 7 we present the upper critical field $H_{c2}(T)$ taken with the criterion 10% ρ_n for the two selected samples with T_c=5.7 K and T_c=3.7 K. One can see that the slope $-d\mu_0 H_{c2}/dT|_{T_c}$ is very different between these two samples. Actually in the previous work of the Princeton group,[9] $-d\mu_0 H_{c2}/dT|_{T_c}$ can be as high as 1 T/K. In a dirty type-II superconductor, it was predicted[18]

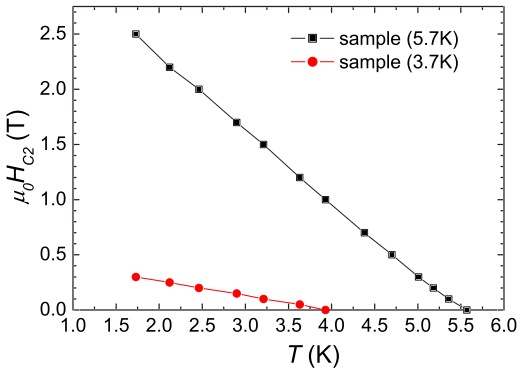

FIG. 7. (Color online) The upper critical field for both samples with different transition temperatures.

that $-d\mu_0 H_{c2}/dT|_{T_c} \propto \rho_n \gamma_n \eta$ with η in connection with the electron-phonon coupling strength. It is thus reasonable to ascribe the variation of $d\mu_0 H_{c2}/dT|_{T_c}$ and T_c to different electron-phonon coupling strengths and different density of states at E_F. All these quantities may be optimized in future work and hopefully will lead to a higher superconducting transition temperature. The basic parameters and properties derived in this work provide a playground for the future study in this interesting system.

V. CONCLUDING REMARKS

In summary, analysis on the low-temperature data in MgIrB finds an *s*-wave pairing symmetry with a gap in the weak coupling to slightly moderate coupling regime and the superconductivity is induced by the electron-phonon coupling. The spin-triplet component, if it exists, should remain as a small part of the total condensate. Tuning the superconducting transition temperature seems possible through changing the electron-phonon coupling strength and the density of states at the Fermi level by varying the relative compositions among the three elements and probably also by mutual substitution.

ACKNOWLEDGMENTS

The authors acknowledge the fruitful discussions with Tao Xiang and Junren Shi at IOP, CAS, and Guoqing Zheng at Okayama University, Japan. This work is supported by the National Science Foundation of China , the Ministry of Science and Technology of China (973 project, Contracts Nos. 2006CB601000 and 2006CB921802), and Chinese Academy of Sciences (project ITSNEM).

*hhwen@aphy.iphy.ac.cn

[1] L. P. Gor'kov and E. I. Rashba, Phys. Rev. Lett. **87**, 037004 (2001).

[2] P. A. Frigeri, D. F. Agterberg, A. Koga, and M. Sigrist, Phys. Rev. Lett. **92**, 097001 (2004).

[3] V. M. Edel'stein, Sov. Phys. JETP **68**, 1244 (1989).

[4] L. S. Levitov, Yu. V. Nazarov, and G. M. Eliashberg, JETP Lett. **41**, 445 (1985).

[5] K. V. Samokhin, E. S. Zijlstra, and S. K. Bose, Phys. Rev. B **69**, 094514 (2004); K. V. Samokhin, E. S. Zijlstra, and S. K. Bose,

Phys. Rev. B **70**, 069902(E) (2004).
[6] N. Hayashi, Y. Kato, P. A. Frigeri, K. Wakabayashi, and M. Sigrist, Physica C **437-438**, 96 (2006).
[7] H. Q. Yuan, D. F. Agterberg, N. Hayashi, P. Badica, D. Vandervelde, K. Togano, M. Sigrist, and M. B. Salamon, Phys. Rev. Lett. **97**, 017006 (2006).
[8] M. Nishiyama, Y. Inada, and Guo-qing Zheng, Phys. Rev. Lett. **98**, 047002 (2007).
[9] T. Klimczuk, Q. Xu, E. Morosan, J. D. Thompson, H. W. Zandbergen, and R. J. Cava, Phys. Rev. B **74**, 220502(R) (2006).
[10] N. R. Werthamer, E. Helfand, and P. C. Hohenberg, Phys. Rev. **147**, 295 (1966).
[11] B. Wiendlocha, J. Tobola, and S. Kaprzyk, arXiv:0704.1295 (unpublished).
[12] H. M. Rosenberg, *Low Temperature Solid State Physics* (Oxford University Press, Oxford, 1963).
[13] N. E. Hussey, Adv. Phys. **51**, 1685 (2002).
[14] K. A. Moler, D. J. Baar, J. S. Urbach, Ruixing Liang, W. N. Hardy, and A. Kapitulnik, Phys. Rev. Lett. **73**, 2744 (1994); K. A. Moler, John R. Kirtley, Ruixing Liang, Douglas Bonn, and Walter N. Hardy, Phys. Rev. B **55**, 12753 (1997).
[15] H. H. Wen, Z. Y. Liu, F. Zhou, J. W. Xiong, W. X. Ti, T. Xiang, S. Komiya, X. F. Sun, and Y. Ando, Phys. Rev. B **70**, 214505 (2004); H. H. Wen, L. Shan, X. G. Wen, Y. Wang, H. Gao, Z. Y. Liu, F. Zhou, J. W. Xiong, and W. X. Ti, *ibid.* **72**, 134507 (2005).
[16] G. E. Volovik, JETP Lett. **58**, 469 (1993).
[17] W. L. McMillan, Phys. Rev. **167**, 331 (1968).
[18] J. E. Jaffe, Phys. Rev. B **40**, 2558 (1989).